

Controlling Fano resonances using the geometrical phase of light in spatially tailored waveguided plasmonic crystals

Subir K. Ray, Ankit K. Singh,^{*} Ajmal, Shubham Chandel, Partha Mitra, and Nirmalya Ghosh

Department of Physical Sciences, Indian Institute of Science Education and Research (IISER) Kolkata, Mohanpur 741246, West Bengal, India



(Received 14 May 2019; published 6 September 2019)

Fano resonance exhibiting an asymmetric spectral line shape is a universal phenomenon observed in diverse physical systems. Here we experimentally establish a direct link between the spectral asymmetry parameter q and a physically realizable phase factor of interference between a continuum and a discrete mode that leads to Fano resonance. We demonstrate control on the spectral asymmetry of the Fano resonance through changes in the geometric phase of polarized light using a specially designed metasurface, namely waveguided plasmonic crystal with a spatially varying orientation axis of the plasmonic grating. In this scenario, the changes in the geometric phase for input left and right circular polarized light arise due to varying orientation angle of the grating axis. The systematic changes in the geometric phase and the resulting q parameter of Fano resonance are interpreted by an appropriate theoretical model connecting the two physical entities. The demonstrated control over the spectral line shape of Fano resonance achieved by tailoring geometric phase may open up routes for polarization-based photonic applications.

DOI: [10.1103/PhysRevA.100.033805](https://doi.org/10.1103/PhysRevA.100.033805)

I. INTRODUCTION

Fano resonance is a ubiquitous interference phenomenon observed in a wide range of physical system including atomic, molecular, nuclear, solid state, as well as in classical optical systems [1–9]. In contrast to the conventional symmetric Lorentzian resonance profile, the Fano resonance is uniquely identified in the spectral line shape as an asymmetric spectral profile where an intensity maximum is immediately followed by an intensity minimum due to destructive interference. The spectral asymmetry emerges due to interference between a continuum mode and a discrete mode, which can be characterized by the asymmetry parameter q [1]. In the optical domain, the asymmetric Fano resonance has been intensively studied not only due to the fundamental interests but also because of its numerous potential applications in sensing, switching, lasing, filters, robust color display, nonlinear and slow-light devices, and so forth [10–21]. In most of the mentioned applications, the ability to control and tune the interference effect with some external parameters is crucial. In the quest of making a suitable structure for a particular application and having high-quality factor resonances in different spectral domains [22–24], various types of metal-dielectric structures like plasmonic oligomers, dolmen, bowtie, split rings, waveguided plasmonic crystal, etc. have been proposed to observe the optical Fano resonances in the scattering or absorption profile [6,9–28].

Despite the availability of voluminous literature on the application aspects of Fano resonance in optical systems, there remain considerable interests in understanding the fundamental nature of this intriguing wave interference phenomenon through some physically meaningful and

experimentally accessible parameters [7,28]. On conceptual and practical grounds such studies are extremely valuable since these not only provide insights and interpretation of the Fano resonance phenomenon, but may also open up novel routes to control and modulate the interference effect and the resulting asymmetric Fano resonance [7,28]. In this regard, we have recently proposed a simple phenomenological model for the electric field scattered from a Fano resonant system and related the spectral asymmetry of the resonance profile (or the q parameter) with a physical parameter: namely, Fano phase shift between the continuum and the discrete mode [28]. Here, we show that the Fano phase shift between the continuum and the discrete mode is indeed a physically meaningful phase factor of light and that this phase factor can be controlled to modulate the Fano q parameter by controlling some degree of freedom of light. We demonstrate this concept in a spatially tailored waveguided plasmonic crystal sample that exhibits Fano resonance due to the spectral interference of a spectrally broad plasmon mode and a narrow waveguide mode. In this particular scenario, the Fano phase factor and the resulting spectral asymmetry parameter is directly related to the Pancharatnam Berry geometric phase of light [29–39], which is systematically changed by varying the orientation axis of the gold grating in the waveguided plasmonic crystal sample. The polarization degree of freedom of light, specifically opposite circular polarization states of light, is subsequently used to probe systematic changes in the Fano spectral line shape of the scattered light as the signature of varying Fano phase shift. The corresponding experimental results are interpreted using a suitable theoretical model, which establishes the link between the Fano phase shift (which is related to geometric phase here) and the asymmetry parameter (q) of Fano resonance. These results uncover an intriguing link between the Fano q parameter and a physically accessible phase of interference and also open up an interesting avenue for control and manipulation

^{*}aks13ip027@iiserkol.ac.in

of optical Fano resonance through a geometrical phase and polarization state of light.

II. THEORY

We first develop a theoretical model that connects the Fano asymmetry parameter q to an additional polarization-dependent geometric phase factor that may arise in an inhomogeneous anisotropic Fano resonant system [29–39]. In the general case, the scattered electric field from a Fano resonant system can be written as the interference of a discrete complex Lorentzian with a continuum of amplitude $B(\omega)$ [28]

$$\mathbf{E}_s \approx \frac{q - i}{\varepsilon + i} + B(\omega) = \frac{\sqrt{q^2 + 1}}{\varepsilon + i} e^{i\psi_f} + B(\omega). \quad (1)$$

Here, $\varepsilon = \varepsilon(\omega) = \frac{\omega - \omega_0}{\gamma/2}$, ω_0 and γ are the central frequency and the width of the discrete mode, respectively, and ψ_f is called the Fano phase factor. Assuming frequency-independent continuum mode, the scattered intensity corresponding to Eq. (1) can be shown to have a spectral intensity component that exhibits a characteristic asymmetric spectral line shape along with a Lorentzian background as [28]

$$I_s = |\mathbf{E}_s|^2 = \frac{(q + B\varepsilon)^2}{\varepsilon^2 + 1} + \frac{(1 - B)^2}{\varepsilon^2 + 1}. \quad (2)$$

If one of the two modes (either discrete or the continuum) has a phase contribution of geometrical origin, the electric field scattered from the mode acquires a geometrical phase ($\sigma\phi_g = \pm\phi_g$) shift for incident LCP or RCP light [30,31,33], depending on the helicity (σ , “ \pm ” is for left or right circular polarization) of the light incident on the Fano resonant scattering system. The origin of this geometrical phase is due to the geometrical orientation of the scattering system with respect to incident polarized light. The scattered electric field from such a Fano resonant system can be written as

$$\mathbf{E}_s \approx \frac{\sqrt{q^2 + 1} e^{i\psi_f}}{\varepsilon + i} + B e^{\pm i\phi_g}. \quad (3)$$

The interference effect gets modulated by the additional geometric phases acquired by the particular mode. The corresponding spectral variation of the intensity for incident LCP or RCP light can be written as

$$I_s^{\text{LCP or RCP}}(\omega, \phi_g) = \frac{[B\varepsilon + (q \cos \phi_g \mp \sin \phi_g)]^2}{\varepsilon^2 + 1} + \frac{[(\cos \phi_g \pm q \sin \phi_g) - B]^2}{\varepsilon^2 + 1}. \quad (4)$$

As evident from Eqs. (3) and (4), the geometric phase of light can modulate the Fano phase shift ψ_f or the resulting asymmetry parameter (q). The difference in the geometrical phase between left and right circular polarization thus leads to a contrast in the scattering spectral line shape for the two polarizations.

III. RESULTS AND EXPERIMENT

In order to probe the circular polarization dependence of the Fano line shape, we took a one-dimensional waveguided

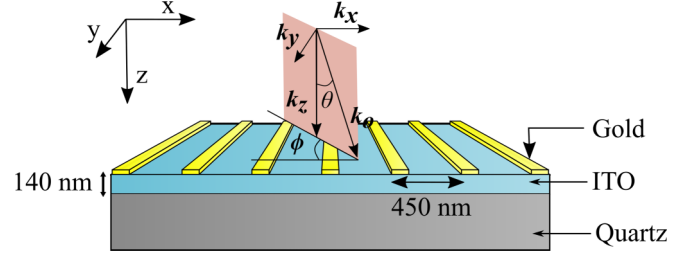


FIG. 1. Schematic of waveguided plasmonic grating crystal. A gold grating of 100 nm width and 20 nm height on top of a 140-nm-thick ITO-coated quartz substrate was taken for the FEM-based COMSOL MULTIPHYSICS simulation. The extinction spectra were studied for light incident at an inclined angle of incidence ($\theta = 16^\circ$) with varying azimuthal angle (ϕ) of incidence from 0° to 90° (in steps of 15°).

plasmonic crystal, a well-studied optical system for the Fano resonance in the extinction spectra [6,9,25,26]. It consists of twofold symmetric one-dimensional gold grating deposited on a thin indium tin oxide (ITO)-coated quartz substrate as shown in Fig. 1. The Fano resonance in such system is observed as a result of interference between a broad dipolar plasmonic resonance of the gold grating and the waveguide mode excited in the ITO layer [6,9,25,26]. It is to be noted that the waveguided plasmonic grating also acts as a diattenuating linear retarder for the electric field incident on the system, showing a simultaneous differential and anisotropic amplitude as well as the phase response for the eigen polarization states [30], as shown later. The orientation axis of the decomposed linear diattenuator and linear phase retarder elements present in the system is decided by the direction of the grating lines and the incident light.

The extinction spectra (defined as extinction = $1 -$ transmission) of a grating (height 20 nm, width 100 nm, and period 450 nm) were calculated at an inclined angle ($\theta = 16^\circ$) with varying the azimuthal angle (ϕ) of incidence from 0° to 90° in steps of 15° , using finite element method (FEM)-based COMSOL MULTIPHYSICS software. The extinction spectra were observed for both the circular polarized input states (i.e., LCP and RCP) with scattered field projected on the input as well as the orthogonal state of circular polarization as shown in Fig. 2. It can be noted from the figure that for an inclined angle of incidence, a differential response of the system for incident LCP or RCP polarizations projected on RCP or LCP polarizations of the transmitted light was observed in the Fano line shape. The origin of such differential response is solely geometric in nature and depends on the orientation angles of the axes of the diattenuating linear retarder (the waveguided plasmonic grating) with the direction of incidence of light giving rise to a geometric phase shift between the plasmonic grating and the waveguide mode. The Fano line shapes were fitted using Eq. (2), and the asymmetry parameter of the resonance was extracted for both polarization projections shown in Fig. 2(b). A clear difference in the asymmetry of the resonances in both polarization was observed for the azimuthal angle of incidence other than 0° and 90° . In order to quantify such polarization projection dependent asymmetry

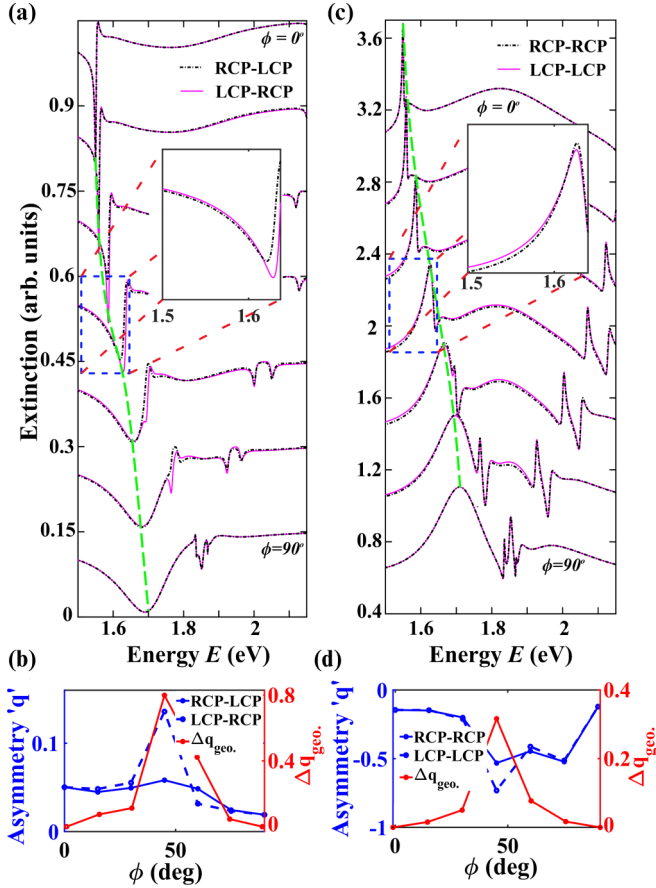


FIG. 2. Dependence of extinction spectra on the azimuthal angle of incidence (ϕ) of a left or right circular polarized light on the grating. (a) Numerically calculated extinction spectra of the grating at inclined angle of incidence ($\theta = 16^\circ$) with varying azimuthal angle of incidence (ϕ) from 0° to 90° in steps of 15° for (a) cross-polarized projections (input RCP polarization projected on LCP and input LCP polarization projected on RCP) and (c) co-polarized projections (input RCP polarization projected on RCP and input LCP polarization on LCP) are shown. The Fano line shape was fitted using Eq. (2) and the asymmetry parameter q (left axis) obtained with varying azimuthal angle is shown for both (b) cross-polarized projections and (d) copolarized projections; a dependence of Δq_{geo} (right axis) with the azimuthal angle (ϕ) is also shown. The findings establish the role of geometric phase on the asymmetry in the extinction spectra.

of the resonance, we defined Δq_{geo} , given as

$$\Delta q_{\text{geo}} = \text{abs} \left(\frac{q_1 - q_2}{q_1 + q_2} \right). \quad (5)$$

Here, q_1 and q_2 are the q values observed for the two circular polarization projections which are being compared. Note that Δq_{geo} depends on the geometry (geometrical orientation) of the anisotropic scattering system as shown in Fig. 2(b). Such dependence of asymmetry of Fano line shape on the azimuthal angle of incidence is a signature of the effect of the geometric phase of light on the Fano line shape with a maximum difference in the asymmetry parameter at $\phi = 45^\circ$ and no difference for $\phi = 0^\circ$ and 90° . It is well known that right and left circularly polarized light acquires equal and

opposite Pancharatnam Berry geometric phases while propagating through an anisotropic medium (phase retarder having linear retardance δ), the magnitude of which depends upon the orientation angle (β) of the anisotropy axis of the medium [30,31,33–35]. It has been argued that the geometric phase in such case should be reflected in the crossed circular polarization component of the transmitted light. Such arguments stem from empirically decomposing the Jones matrix of a phase retarder as a coherent sum of the Jones matrices of a half-wave retarder ($\delta = \pi$) and an identity matrix [35]. However, we would like to note that such decomposition is strictly valid for a half-wave retarder only. On the other hand, for an arbitrary linear retarder (with retardance $\delta \neq \pi$) or diattenuating linear retarder, the dependence of the geometric phase on the orientation angle of the axis of the retarder [32], and the projection polarization state is rather complex [32,36–39].

The Jones matrix of a diattenuating retarder $J = J_R J_D$ can be written as a product of the Jones matrix of a diattenuator (J_D) and a retarder (J_R). In case of the waveguided plasmonic grating, the diattenuation primarily arises because of the differential amplitude response of the waveguiding layer whereas the retardance originates due to differential phase response of the plasmonic grating for the eigen polarization states. In such scenario, the axis (eigenvectors) of the polarization diattenuator is determined by the angle of inclination of the incident light with respect to the waveguide layer, whereas the axis of retarder is determined by the orientation angle of grating with the incident light. In such case the Jones matrix of system becomes inhomogeneous, i.e., have nonorthogonal eigenvectors (\mathbf{E}_g and \mathbf{E}_h , with eigenvalues μ_g and μ_h , respectively) and the total phase difference between the input (\mathbf{E}_a) and output ($\mathbf{E}_b = J\mathbf{E}_a$) can be given as [36,37]

$$\Phi = \arg \left[\mu_g + \mu_h + (\mu_g - \mu_h) \frac{\mathbf{E}_g \cdot (\boldsymbol{\Sigma}_3 (\boldsymbol{\Sigma} \cdot \mathbf{S}_a) \mathbf{E}_h)}{\mathbf{E}_g \cdot (\boldsymbol{\Sigma}_3 \mathbf{E}_h)} \right]. \quad (6)$$

Here, ($\boldsymbol{\Sigma} = \boldsymbol{\Sigma}_1, \boldsymbol{\Sigma}_2, \boldsymbol{\Sigma}_3$) denotes the three Pauli matrices and \mathbf{S}_a denotes the normalized Stokes vector of input state. In the above formulation [Eq. (6)] of the Jones matrix of the diattenuating retarder system there is no total dynamical phase acquired as $\arg(\det(J)) = 0$ [36,37]. Thus, the total phase acquired by the system is solely geometrical in nature ($\phi_g = \Phi$). Using the above equation it can be shown that even in a simple diattenuating retarder system, there is a geometric phase difference acquired between incident RCP or LCP ($\mathbf{E}_a = [1 \pm i]$) polarization states and the transmitted elliptical polarized light (\mathbf{E}_b) for varying orientation axis of the retarder (see Supplemental Material) [36,37,40]. In such scenario, projection of the elliptical state coming out of the diattenuating retarder system to a different polarization states leads to acquisition of different geometrical phases. Thus an orientation angle (of the axis of the retarder) dependent geometric phase is obtained from the anisotropic system which gets reflected in the cross- as well as cocircularly polarized component of the light transmitted from the system [32,36,37]. In Fig. 2(c), we have shown the extinction cross section from the sample for incident LCP or RCP polarization with the light transmitted from the sample being projected on the same polarization, i.e., LCP or RCP. It can be noted from the figure that the system shows a differential response for the two polarization projections similar to the earlier case. These results clearly

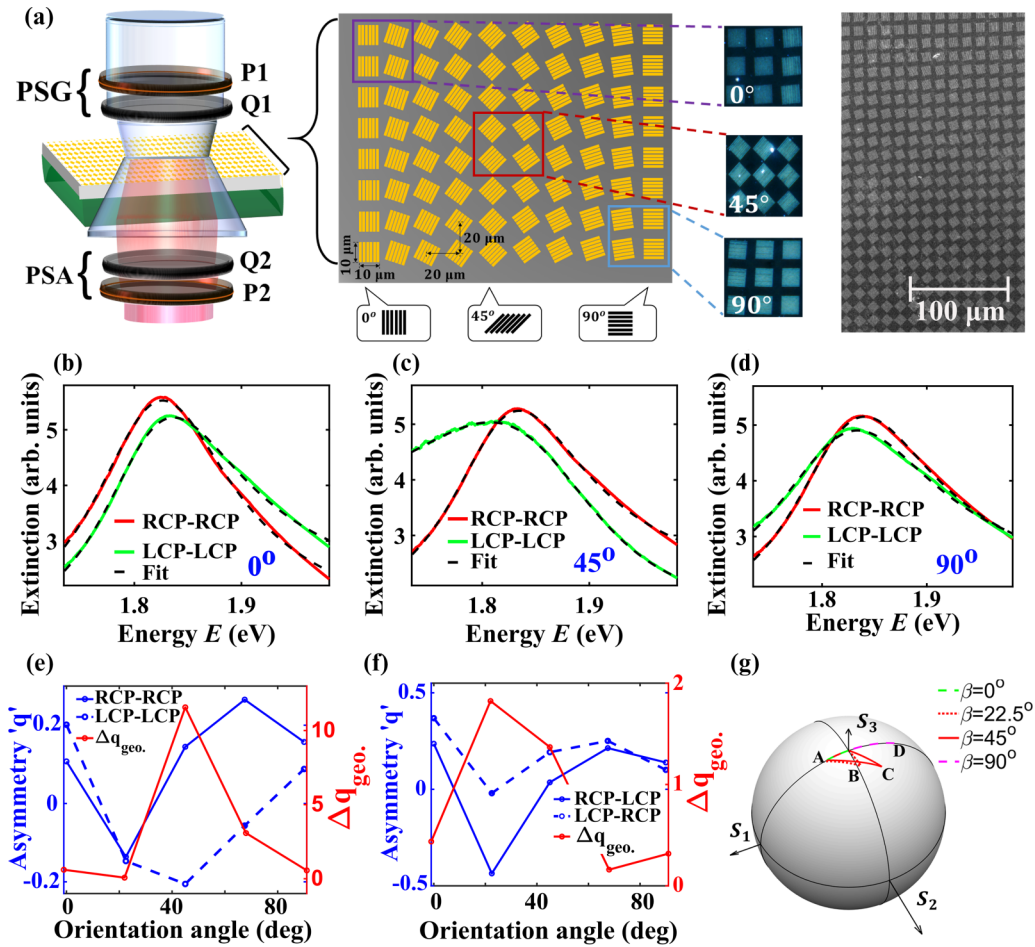


FIG. 3. Geometric phase-controlled tuning of extinction spectra for spatially tailored waveguided plasmonic crystals. (a) Schematic of a dark-field microscope integrated with a polarization state generator and polarization state analyzer units. The inset shows the dark-field images of the plasmonic grating for orientation angles of 0° , 45° , and 90° , respectively, and the SEM image of the spatially tailored waveguided plasmonic crystals. (b)–(d) The corresponding spectral response for the copolarized projections of the plasmonic grating system oriented at angles of 0° , 45° , and 90° are shown, respectively. The dependence of the asymmetry parameter q (left axis, blue lines) with the grating orientation angle for (e) the copolarized projections (LCP projected on LCP, and RCP projected on RCP) and (f) the cross-polarized projections (LCP projected on RCP, and RCP projected on LCP) are shown; a dependence of Δq_{geo} (right axis) with the orientation is also shown. The dependence of the asymmetry of resonance on the geometrical orientation of the plasmonic grating clearly shows the role of the geometric phase of light in tuning the Fano phase. (g) The trajectory of polarization evolution on Poincaré sphere for different orientation of the angle ($\beta = 0^\circ, 22.5^\circ, 45^\circ$, and 90°) of the grating axis (with retardance $\delta \approx 0.30$ rad and diattenuation $d \approx 0.25$); the points A, B, C, and D on Poincaré sphere represent the elliptical state after pass through the diattenuating retarder for different orientation of the retarder axis.

illustrate that indeed a geometrical phase is acquired even in the copolarized polarization projections [32,36,37]. In what follows, we experimentally demonstrate that the geometric phase can indeed be used for tuning the asymmetry of Fano line shape of spatially tailored waveguided plasmonic crystals having a spatially varying axis of the gratings.

In Fig. 3(a), we have shown a schematic of our experimental setup. A dark-field microscope integrated with a polarization-state generator (PSG) unit and a polarization-state analyzer (PSA) unit. The PSG unit consists of a polarizer (P1) followed by a quarter-wave plate (Q1) to generate an arbitrary state of polarization, and these elements are arranged in reverse order in the PSA unit to analyze an arbitrary state of polarization. The annular illumination of the dark-field microscope [27,28,41] was used to record the scattered-field spectral response from the spatially tailored waveguided plasmonic crystals [shown in scanning electron microscope

(SEM) image] for grating orientated at a particular orientation (shown in the dark-field images). The spatially tailored waveguided plasmonic crystal consist of $10\text{-}\mu\text{m} \times 10\text{-}\mu\text{m}$ gold gratings of height 22 nm, width 80 nm, and a period 550 nm deposited on top of 190-nm-thick ITO coated quartz substrate. The separation between the individual gratings was kept $20\text{ }\mu\text{m}$ in x and y directions to avoid any overlap (as shown in the schematic), with a desirably varying orientation angles of the plasmonic gratings axis (as shown in the schematic). For the microscopic polarization investigation, a nanotranslation stage was used to move the sample in the illumination focal plane of the microscope such that only a small region of the plasmonic crystal gets illuminated by the light [as shown in the inset dark-field images in Fig. 3(a)].

Regions with different orientation angles of the axis of the plasmonic grating were experimentally studied by illuminating and collecting from different regions of the grating using a

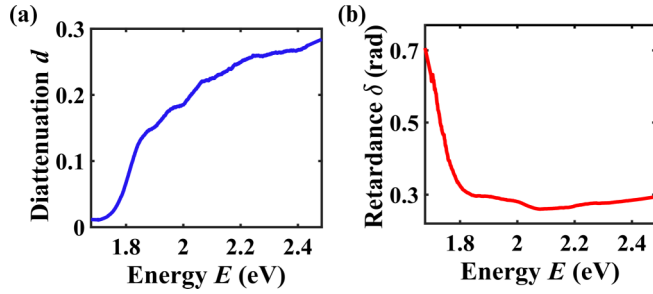


FIG. 4. Polarization parameters linear diattenuation (d) and linear retardance (δ) extracted from the Mueller matrix of a waveguided plasmonic grating crystal. (a) Diattenuation (d) parameter showing small-amplitude anisotropy ($d \approx 0.25$) and (b) linear retardance (δ) parameter showing small-phase anisotropy ($\delta \approx 0.3$) of the waveguided plasmonic grating.

nanotranslation stage with a fixed incident light. This enabled collection of scattered light intensity separately from various different orientation angle regions of the grating. It can be noted from the inset dark-field images that the light can be focused such that we get scattering from grating oriented at a particular angle and the annular illumination in the dark-field microscopic configuration leads to an inclined illumination of the waveguided plasmonic grating sample as opposed to exact normal illumination [27,28,41]. The situation is analogous to the case when light with varying azimuthal angle is incident on the waveguided plasmonic grating with the orientation axis of the plasmonic grating fixed as shown in simulations. The field scattered from the illuminated portion is collected through a spectrometer after passing through the PSA unit. The PSA and PSG units were used to record the scattering spectra for both circular polarization input as well as output combinations with different orientation angles of the grating as shown in Fig. 3. It can be noted from the figure that a significant amount of change in the asymmetry parameter (q) of line shape (obtained by fitting the spectrum with Eq. (2)) is observed with different orientation angles (β) of grating for both co- and cross-polarized polarization projections as shown in Figs. 3(e) and 3(f). The variation of Δq_{geo} parameter with the orientation angle (β) of the grating shows that the geometric phase of light indeed modulates the asymmetry of the Fano resonance line shape. In Fig. 3(g), we show the expected trajectory of the polarization state of light on the Poincaré sphere when incident right circularly polarized light passes through the diattenuating retarder system and is subsequently projected to the same right circular polarization state. The results are shown for four different orientation angles of the retarder axis (β) and a fixed diattenuator axis (see Supplemental Material [40]). For simulating this trajectory the diattenuation ($d \approx 0.25$) and the retardance ($\delta \approx 0.30$) polarization parameters were taken that are close to our experimental values of these polarization parameters for the waveguided plasmonic crystal sample (shown subsequently in Fig. 4). Clearly, the path of the polarization evolution (area enclosed) changes with varying orientation angle of the grating, demonstrating evolution of different geometrical phases even for copolarized projections [32,36,37].

We recorded the full polarization response of the grating for one such axial orientation in the form of the Mueller

matrix of the waveguided grating sample (see Supplemental Material [40]). The recorded Mueller matrix was used to extract the linear diattenuation (d) and linear retardance (δ) parameters of the grating shown in Fig. 4. It can be noted from the figure that the plasmonic grating system indeed acts as a diattenuating retarder with a small phase retardance value ($\delta \approx 0.30$ rad) and a small linear diattenuation ($d \approx 0.25$) in scattering from the system.

IV. DISCUSSION

It is well known that the Pancharatnam Berry geometric phase acquired by circularly (or elliptically) polarized light while propagating through an anisotropic medium exhibiting linear retardance effect depends upon the orientation angle of the axis of retarder [30–35]. In the simplest case of a pure half-wave retarder ($\delta = \pi$), the acquired geometric phase ϕ_g has a rather simple dependence on the orientation angle $\phi_g = 2\sigma\beta$ [30,31,33–35]. As previously discussed, in such case, empirically it has been shown that the resulting geometrical phase gets accumulated in the cross-polarized component of incident circular polarized light [30–35]. However, the situation can be complex for arbitrary diattenuating retarder ($\delta \neq \pi$, $d \neq 0$), as evident from the results presented in Figs. 2 and 3. In such case, the polarization evolution follows a trajectory on the Poincaré sphere which depends on the orientation axis of diattenuator and retarder elements as well as their strengths [as shown Fig. 3(g)] [32,36–39]. Nevertheless, the geometric phase acquired by left or right circularly polarized light while propagating through an arbitrary diattenuating retarder system depends upon the orientation angle of the anisotropy axes. Thus, despite the ensuing complexities on the dependence of the geometric phase on the orientation angle, the results presented in Figs. 2 and 3 clearly demonstrate that the spectral asymmetry of Fano resonance in our diattenuating retarder system of waveguided plasmonic crystal is related to the geometric phase of light that evolves due to the interaction of polarized light with such system. These results validate the physical nature of the phase shift of Fano interference and its connection with the spectral asymmetry of Fano resonance. It also demonstrates that the polarization-tuned geometrical phase of light can be used to modulate the spectral line shape of Fano resonance in an appropriately designed anisotropic Fano resonant system.

V. CONCLUSION

In conclusion, we have demonstrated a fundamentally interesting concept associated with Fano resonance by establishing and demonstrating a relationship between the Fano spectral asymmetry parameter q and a physical phase shift of Fano interference between a continuum and a narrow resonance mode. Using geometric phase metasurface of waveguided plasmonic crystal, we have experimentally demonstrated control over this phase shift and the resulting asymmetry of Fano spectral line shape through a polarization-tuned geometrical phase of light. The experimental results are supported further by the results of FEM-based COMSOL simulations. In the

process, the results of these studies also uncover insights on the dependence of geometric phase of light on the orientation angle of anisotropy axis of arbitrary diattenuating retarder and the projection polarization state of light. The finding can open up discussions to study such dependence. The results reveal that the Fano q parameter can be controlled by a physically accessible phase of interference; the findings illustrate that the geometrical phase and polarization state of light can be used as an additional degree of freedom to control and manipulate the Fano resonance

ACKNOWLEDGMENTS

The authors acknowledge the Indian Institute of Science Education and Research, Kolkata for the funding and facilities. S.K.R. acknowledges financial support from the University Grants Commission (UGC), Government of India through a research fellowship. A.K.S. acknowledges financial support from the Council of Scientific and Industrial Research (CSIR), Government of India through a research fellowship.

S.K.R. and A.K.S. contributed equally to this work.

-
- [1] U. Fano, Effects of configuration interaction on intensities and phase shifts, *Phys. Rev.* **124**, 1866 (1961).
- [2] A. C. Johnson, C. M. Marcus, M. P. Hanson, and A. C. Gossard, Coulomb Modified Fano Resonance in a One-Lead Quantum Dot, *Phys. Rev. Lett.* **93**, 106803 (2004).
- [3] I. Mazumdar, A. R. P. Rau, and V. S. Bhasin, Efimov States and Their Fano Resonances in a Neutron-Rich Nucleus, *Phys. Rev. Lett.* **97**, 062503 (2006).
- [4] A. R. Schmidt, M. H. Hamidian, P. Wahl, F. Meier, A. V. Balatsky, J. D. Garrett, T. J. Williams, G. M. Luke, and J. C. Davis, Imaging the Fano lattice to ‘hidden order’ transition in URu₂Si₂, *Nature (London)* **465**, 570 (2010).
- [5] P. Fan, Z. Yu, S. Fan, and M. L. Brongersma, Optical Fano resonance of an individual semiconductor nanostructure, *Nat. Mater.* **13**, 471 (2014).
- [6] B. Luk’yanchuk, N. I. Zheludev, S. A. Maier, N. J. Halas, P. Nordlander, H. Giessen, and C. T. Chong, The Fano resonance in plasmonic nanostructures and metamaterials, *Nat. Mater.* **9**, 707 (2010).
- [7] C. Ott, A. Kaldun, P. Raith, K. Meyer, M. Laux, J. Evers, C. H. Keitel, C. H. Greene, and T. Pfeifer, Lorentz meets Fano in spectral line shapes: A universal phase and its laser control, *Science* **340**, 716 (2013).
- [8] Y. Sonnefraud, N. Verellen, H. Sobhani, G. A. E. Vandenbosch, V. V. Moshchalkov, P. V. Dorpe, P. Nordlander, and S. A. Maier, Experimental realization of subradiant, superradiant, and Fano resonances in ring/disk plasmonic nanocavities, *ACS Nano* **4**, 1664 (2010).
- [9] A. Christ, S. G. Tikhodeev, N. A. Gippius, J. Kuhl, and H. Giessen, Waveguide Plasmon Polaritons: Strong Coupling of Photonic and Electronic Resonances in a Metallic Photonic Crystal Slab, *Phys. Rev. Lett.* **91**, 183901 (2003).
- [10] J. N. Anker, W. P. Hall, O. Lyandres, N. C. Shah, J. Zhao, and R. P. V. Duyne, Biosensing with plasmonic nanosensors, *Nat. Mater.* **7**, 442 (2008).
- [11] W.-S. Chang, J. B. Lassiter, P. Swanglap, H. Sobhani, S. Khatua, P. Nordlander, N. J. Halas, and S. Link, A plasmonic Fano switch, *Nano Lett.* **12**, 4977 (2012).
- [12] A. Bärnthaler, S. Rotter, F. Libisch, J. Burgdörfer, S. Gehler, U. Kuhl, and H.-J. Stöckmann, Probing Decoherence Through Fano Resonances, *Phys. Rev. Lett.* **105**, 056801 (2010).
- [13] C. Wu, A. B. Khanikaev, R. Adato, N. Arju, A. A. Yanik, H. Altug, and G. Shvets, Fano-resonant asymmetric metamaterials for ultrasensitive spectroscopy and identification of molecular monolayers, *Nat. Mater.* **11**, 69 (2012).
- [14] K. Nozaki, A. Shinya, S. Matsuo, T. Sato, E. Kuramochi, and M. Notomi, Ultralow-energy and high-contrast all-optical switch involving Fano resonance based on coupled photonic crystal nanocavities, *Opt. Express* **21**, 11877 (2013).
- [15] A. Kaldun, C. Ott, A. Blättermann, M. Laux, K. Meyer, T. Ding, A. Fischer, and T. Pfeifer, Extracting Phase and Amplitude Modifications of Laser-Coupled Fano Resonances, *Phys. Rev. Lett.* **112**, 103001 (2014).
- [16] M. R. Shcherbakov, P. P. Vabishchevich, V. V. Komarova, T. V. Dolgova, V. I. Panov, V. V. Moshchalkov, and A. A. Fedyanin, Ultrafast Polarization Shaping with Fano Plasmonic Crystals, *Phys. Rev. Lett.* **108**, 253903 (2012).
- [17] C. Wu, A. B. Khanikaev, and G. Shvets, Broadband Slow Light Metamaterial Based on a Double-Continuum Fano Resonance, *Phys. Rev. Lett.* **106**, 107403 (2011).
- [18] B. Zhang, Electrodynamics of transformation-based invisibility cloaking, *Light: Sci. Appl.* **1**, e32 (2012).
- [19] N. I. Zheludev, S. L. Prosvirnin, N. Papisimakis, and V. A. Fedotov, Lasing spaser, *Nat. Photonics* **2**, 351 (2008).
- [20] Y. Zhu, X. Hu, Y. Huang, H. Yang, and Q. Gong, Fast and low-power all-optical tunable Fano resonance in plasmonic microstructures, *Adv. Opt. Mater.* **1**, 61 (2013).
- [21] E. Kamenetskii, A. Sadreev, and A. Miroshnichenko, *Fano Resonances in Optics and Microwaves* (Springer, Heidelberg, 2018).
- [22] R. Singh, I. Al-Naib, W. Cao, C. Rockstuhl, M. Koch, and W. Zhang, The Fano resonance in symmetry broken terahertz metamaterials, *IEEE Trans. Terahertz Sci. Technol.* **3**, 820 (2013).
- [23] Y. Fan, Z. Wei, H. Li, H. Chen, and C. M. Soukoulis, Low-loss and high-Q planar metamaterial with toroidal moment, *Phys. Rev. B* **87**, 115417 (2013).
- [24] V. A. Fedotov, M. Rose, S. L. Prosvirnin, N. Papisimakis, and N. I. Zheludev, Sharp Trapped-Mode Resonances in Planar Metamaterials with a Broken Structural Symmetry, *Phys. Rev. Lett.* **99**, 147401 (2007).
- [25] A. Barbara, P. Quémerais, E. Bustarret, T. López-Rios, and T. Fournier, Electromagnetic resonances of sub-wavelength rectangular metallic gratings, *Eur. Phys. J. D* **23**, 143 (2003).
- [26] A. Christ, T. Zentgraf, J. Kuhl, S. G. Tikhodeev, N. A. Gippius, and H. Giessen, Optical properties of planar metallic photonic crystal structures: Experiment and theory, *Phys. Rev. B* **70**, 125113 (2004).
- [27] S. Chandel, A. K. Singh, A. Agrawal, K. A. Aneeth, A. Gupta, A. Venugopal, and N. Ghosh, Mueller matrix spectroscopy of

- Fano resonance in plasmonic oligomers, *Opt. Commun.* **432**, 84 (2019).
- [28] S. K. Ray, S. Chandel, A. K. Singh, A. Kumar, A. Mandal, S. Misra, P. Mitra, and N. Ghosh, Polarization tailored Fano interference in plasmonic crystals: A Mueller matrix model of anisotropic Fano resonance, *ACS Nano* **11**, 1641 (2017).
- [29] S. Pancharatnam, Generalized theory of interference and its applications, *Proc.- Indian Acad. Sci., Sect. A* **44**, 247 (1956).
- [30] S. D. Gupta, N. Ghosh, and A. Banerjee, *Wave Optics: Basic Concepts and Contemporary Trends* (CRC Press, Boca Raton, FL, 2015).
- [31] R. Bhandari, Polarization of light and topological phases, *Phys. Rep.* **281**, 1 (1997).
- [32] R. Bhandari, SU (2) phase jumps and geometric phases, *Phys. Lett. A* **157**, 2211991.
- [33] Z. E. Bomzon, G. Biener, V. Kleiner, and E. Hasman, Space-variant Pancharatnam–Berry phase optical elements with computer-generated subwavelength gratings, *Opt. Lett.* **27**, 1141 (2002).
- [34] L. Marrucci, C. Manzo, and D. Paparo, Optical Spin-to-Orbital Angular Momentum Conversion in Inhomogeneous Anisotropic Media, *Phys. Rev. Lett.* **96**, 163905 (2006).
- [35] X. Ling, X. Zhou, K. Huang, Y. Liu, C. W Qiu, H. Luo, and S. Wen, Recent advances in the spin Hall effect of light, *Rep. Prog. Phys.* **80**, 066401 (2017).
- [36] D. Lopez-Mago, A. Canales-Benavides, R. I. Hernandez-Aranda, and J. C. Gutiérrez-Vega, Geometric phase morphology of Jones matrices, *Opt. Lett.* **42**, 2667 (2017).
- [37] J. C. Gutiérrez-Vega, Pancharatnam–Berry phase of optical systems, *Opt. Lett.* **36**, 1143 (2011).
- [38] T. Van Dijk, H. F. Schouten, and T. D. Visser, Geometric interpretation of the Pancharatnam connection and non-cyclic polarization changes, *J. Opt. Soc. Am. A* **27**, 1972 (2010).
- [39] J. Lages, R. Giust, and J. M. Vigoureux, Geometric phase and Pancharatnam phase induced by light wave polarization, *Physica E* **59**, 6 (2014).
- [40] See Supplemental Material at <http://link.aps.org/supplemental/10.1103/PhysRevA.100.033805> for a description of the origin of the geometric phase in the diattenuating retarder system for various values of the parameters. It also discusses the strategy to record the Mueller matrix of a scattering sample. The Mueller matrix of a waveguided plasmonic grating sample used to extract the polarization parameters is shown.
- [41] S. Chandel, J. Soni, S. K. Ray, A. Das, A. Ghosh, S. Raj, and N. Ghosh, Complete polarization characterization of single plasmonic nanoparticle enabled by a novel dark-field Mueller matrix spectroscopy system, *Sci. Rep.* **6**, 26466 (2016).